A) Cynthia C. Gilmour, Dwayne A. Elias, Amy M. Kucken, Steven D. Brown, Anthony V. Palumbo, Christopher W. Schadt, and Judy D. Wall (2011) Sulfate-Reducing Bacterium Desulfovibrio desulfuricans ND132 as a Model for Understanding Bacterial Mercury Methylation. Appl Environ Microbiol. 77(12): 3938–3951. doi: 10.1128/AEM.02993-10

ABSTRACT

We propose the use of *Desulfovibrio desulfuricans* ND132 as a model species for understanding the mechanism of microbial Hg methylation. Strain ND132 is an anaerobic dissimilatory sulfate-reducing bacterium (DSRB), isolated from estuarine mid-Chesapeake Bay sediments. It was chosen for study because of its exceptionally high rates of Hg methylation in culture and its metabolic similarity to the lost strain *D. desulfuricans* LS, the only organism for which methylation pathways have been partially defined. Strain ND132 is an incomplete oxidizer of short-chain fatty acids. It is capable of respiratory growth using fumarate as an electron acceptor, supporting growth without sulfide production. We used enriched stable Hg isotopes to show that ND132 simultaneously produces and degrades methylmercury (MeHg) during growth but does not produce elemental Hg. MeHg produced by cells is mainly excreted, and no MeHg is produced in spent medium. Mass balances for Hg and MeHg during the growth of cultures, including the distribution between filterable and particulate phases, illustrate how medium chemistry and growth phase dramatically affect Hg solubility and availability for methylation. The available information on Hg methylation among strains in the genus *Desulfovibrio* is summarized, and we present methylation rates for several previously untested species. About 50% of *Desulfovibrio* strains tested to date have the ability to produce MeHg. Importantly, the ability to produce MeHg is constitutive and does not confer Hg resistance. A 16S rRNA-based alignment of the genus *Desulfovibrio* allows the very preliminary assessment that there may be some evolutionary basis for the ability to produce MeHg within this genus.

This work was supported by the U.S. Department of Energy under the Subsurface Biogeochemical Research Program (SBR), Office of Biological and Environmental Research, Office of Science, in part through the Mercury Science Focus Area Program at Oak Ridge National Laboratory (ORNL), through DE-**FG02-07ER64396 (J.D.W.),** by National Science Foundation grant DEB0351050 (C.C.G.), and by the SERC Research Experience for Undergraduates program. ORNL is managed by University of Tennessee UT—Battelle, LLC, for the Department of Energy under contract no. DE-AC05-00OR22725.

B) Steven D. Brown[1], Cynthia C. Gilmour, Amy M. Kucken, Judy D. Wall, Dwayne A. Elias, Craig C. Brandt, Mircea Podar, Olga Chertkov, Brittany Held, David C. Bruce, John C. Detter, Roxanne Tapia, Cliff S. Han, Lynne A. Goodwin, Jan-Fang Cheng, Samuel Pitluck, Tanja Woyke, Natalia Mikhailova, Natalia N. Ivanova, James Han, Susan Lucas, Alla L. Lapidus, Miriam L. Land, Loren J. Hauser and Anthony V. Palumbo. (2011) Genome Sequence of the Mercury-Methylating Strain Desulfovibrio desulfuricans ND132. J. Bacteriol. 193:2078-2079. doi: 10.1128/JB.00170-11

ABSTRACT

Desulfovibrio desulfuricans strain ND132 is an anaerobic sulfate-reducing bacterium (SRB) capable of producing methylmercury (MeHg), a potent human neurotoxin. The mechanism of methylation by this and other organisms is unknown. We present the 3.8-Mb genome sequence to provide further insight into microbial mercury methylation.

This research was supported by the Office of Biological and Environmental Research (OBER), Office of Science, U.S. Department of Energy (DOE), as part of the Mercury Science Focus Area Program at Oak Ridge National Laboratory and **grant DE-FG02-073464396 (J.D.W.).** Oak Ridge National Laboratory is managed by UT-Battelle, LLC, for the U.S. Department of Energy under contract DE-AC05-00OR22725. The work conducted by the U.S. Department of Energy Joint Genome Institute is supported by the Office of Science of the U.S. Department of Energy under contract no. DE-AC02-05CH11231.

C) Jerry M. Parks1, Alexander Johs, Mircea Podar, Romain Bridou, Richard A. Hurt Jr, Steven D. Smith, Stephen J. Tomanicek, Yun Qian, Steven D. Brown, Craig C. Brandt, Anthony V. Palumbo, Jeremy C. Smith, Judy D. Wall, Dwayne A. Elias, and Liyuan Liang (2013) The Genetic Basis for Bacterial Mercury Methylation. Science Vol. 339 no. 6125 pp. 1332-1335 DOI: 10.1126/science.1230667

ABSTRACT

Methylmercury is a potent neurotoxin produced in natural environments from inorganic mercury by anaerobic bacteria. However, until now the genes and proteins involved have remained unidentified. Here, we report a two-gene cluster, *hgcA* and *hgcB*, required for mercury methylation by *Desulfovibrio desulfuricans* ND132 and *Geobacter sulfurreducens* PCA. In either bacterium, deletion of *hgcA*, *hgcB*, or both genes abolishes mercury methylation. The genes encode a putative corrinoid protein, HgcA, and a 2[4Fe-4S] ferredoxin, HgcB, consistent with roles as a methyl carrier and an electron donor required for corrinoid cofactor reduction, respectively. Among bacteria and archaea with sequenced genomes, gene orthologs are present in confirmed methylators but absent in nonmethylators, suggesting a common mercury methylation pathway in all methylating bacteria and archaea sequenced to date.

Supported by the U.S. Department of Energy (DOE), Office of Science, Office of Biological and Environmental Research, through the Mercury Scientific Focus Area Program at Oak Ridge National Laboratory (ORNL). ORNL is managed by UT Battelle, LLC, for DOE under contract DE-AC05-00OR22725 **[My error was not attributing the current grant which was clearly necessary for this work to come to fruition!]**

Steven D. Smith [1], Romain Bridou [1], Alexander Johs [2], Jerry M. Parks [3], Dwayne A. Elias [3,4], Richard A. Hurt [3], Steven D. Brown [3,4], Mircea Podar [2,5], Judy D. Wall [1,#]

[1] Department of Biochemistry, University of Missouri, Columbia, MO, USA. [2]Environmental Sciences Division, Oak Ridge National Laboratory, Oak Ridge, TN, USA. [3]Biosciences Division, Oak Ridge National Laboratory, Oak Ridge, TN, USA. [4]Department of Biochemistry and Cellular and Molecular Biology, University of Tennessee, Knoxville, TN, USA. [5]Department of Microbiology, University of Tennessee, Knoxville, TN, USA.

Running title: Residues of HgcA and HgcB important for Hg(II) methylation

Prepared for submission to *Applied and Environmental Microbiology*

#Address correspondence to: Judy D. Wall, wallj@missouri.edu

Abstract (245 words- 250 words max)

Methylmercury is a potent neurotoxin produced by microorganisms. However, the biochemical mechanism by which anaerobic microorganisms convert inorganic mercury to methylmercury was unknown until recently, when it was shown that a two-gene cluster, consisting of *hgcA* and *hgcB,* encodes the proteins responsible. *hgcA* encodes a corrinoid protein with a strictly conserved cysteine proposed to be a ligand for the cobalt in the corrinoid cofactor. *hgcB* encodes a ferredoxin-like protein thought to be an electron donor to HgcA. When either of these genes was deleted in the methylating bacterium *Desulfovibrio desulfuricans* ND132, mercury methylation was eliminated. Additional mutation strategies were used to determine amino acid residues or regions in HgcA and HgcB essential for the mercury methylation reaction and to test predictions of function derived from structural modeling. Mutations of the conserved cysteine-93, the proposed ligand for the corrinoid cobalt, completely obliterated methylation capacity. Other nearby conserved amino acids, when mutated, had differing effects on methylation capacity but showed that the structure of the 'cap helix' region harboring cysteine-93 is more important than the chemistry conveyed by the particular amino acid residues. In the ferredoxin-like protein HgcB, vicinal cysteines at the C-terminus are highly conserved. Only one of two cysteines was found to be necessary for methylation, but either will suffice. This study supports the previously predicted importance of cysteine-93 for methylation and adds new information about the enzymes, revealing key residues of HgcA and HgcB that facilitate methylation of mercury through catalysis or structural maintenance.

Introduction

Methylmercury (MeHg), a neurotoxin present in the environment, represents a significant risk to human health in many regions of the world (1). Currently only anaerobic microbes are known to produce MeHg biotically (2), predominantly in sediments of aquatic environments. Sources of the mercury (Hg(II)) substrate from which MeHg is derived are numerous and include natural as well as anthropogenic sources (3, 4). In 2013, recognizing that Hg and, therefore, MeHg in the global environment remain a growing problem, countries from across the globe met to sign the Minamata Convention to limit anthropogenic mercury emissions. (http://www.mercuryconvention.org/News/GlobalTreatyonMercuryPollutionGetsBoostfrom/tabid/3524/Default.aspx) This international attention confirms that Hg and MeHg in the environment represent an urgent, prominent human health problem that must be addressed.

Once MeHg has been produced by sediment microorganisms, it accumulates in the aquatic food chain, becoming concentrated in top predators (5). MeHg exposure to humans results from eating the top predators of marine food webs, such as shark, albacore tuna, and eel that are widely consumed by people of all demographics. Once in the body, MeHg passes through the intestinal epithelium, usually complexed with thiol groups in proteins (6). Eventually MeHg buildup in humans can lead to neuropathies in the adult and developmental disorders in children exposed *in utero* (3).

Anaerobic δ-proteobacteria are thought to be the major contributors to MeHg found in the environment (7-9), although the potential contribution of methanogens has recently been discovered (9, 10). In 2013, Parks et al. (11) showed that the proteins encoded by the genes

hgcA and *hgcB* are essential for the conversion of Hg(II) to $MeHg^{+}$. The Parks et al. study was stimulated by the description of Bartha and colleagues (12-14) of a 40-kD corrinoid protein implicated in methylation of Hg(II) in protein extracts of *Desulfovibrio desulfuricans* LS, a strain that was subsequently lost. Hg(II) methylation was thought to involve the reductive acetyl-CoA pathway and perhaps the corrinoid protein therein (13, 15). With this information as a starting point, along with the genome sequences of a small number of bacteria known to methylate Hg(II), the amino acid sequence of the corrinoid iron sulfur protein (CFeSP) from the reductive acetyl-CoA pathway of *Carboxydothermus hydrogenoformans* Z-2901 (16, 17) was used to search the proteins predicted from the genomes of known Hg(II) methylators. By comparing sequences of Hg(II) methylating and non-methylating bacteria, these researchers identified a gene conserved in all methylators, absent in non-methylators, that appeared to encode a corrinoid protein of the approximate size of that reported by Choi and Bartha in 1993. This gene was subsequently shown by mutational studies in *Desulfovibrio desulfuricans* ND132 (ND132) and *Geobacter sulfurreducens* PCA to be essential for Hg(II) methylation and was designated *hgcA* (11).

Immediately downstream (14 bp) from *hgcA* in the ND132 genome there is a predicted gene encoding a ferredoxin-like protein that was also shown to be essential for Hg(II) methylation (11). Therefore, this gene was named *hgcB*. It was hypothesized that the two genes, essential for methylation and occurring in close proximity in the genome, produce proteins that likely work together in the Hg(II) methylation reaction.

Both *hgcA* and *hgcB* homologues have since been identified in other organisms of diverse origins and environments. All microbes assayed thus far that have *hgcA* and *hgcB* methylate Hg(II). All microbes assayed that lack homologues of *hgcA* and *hgcB* have been shown to be unable to methylate Hg(II)(18).

Although initial work has identified genes essential for Hg(II) methylation, proof is lacking that the bioinformatics and modeling predictions of the critical residues involved in the methylation reaction are correct. The structure of CFeSP, a two subunit complex of CfsA and CfsB, from *C. hydrogenoformans* ($CFeSP_{Ch}$) that was used for identification of HgcA, was initially determined by Svetlitchnaia et.al. (17). The large subunit of $CFeSP_{Ch}$, CfsA containing the corrinoid cofactor, has several features not shared with HgcA. CfsA has three domains, an N-terminal domain binding a single [4Fe-4S] center, a $(\beta\alpha)_8$- barrel in a middle domain, and a C-terminal domain that binds the corrinoid 5,6- dimethylbenzimidazolylcobamide in a "base-off" configuration. The smaller, single domain subunit of $CFeSP_{Ch}$, CfsB, folds as a $(\beta\alpha)_8$- barrel and interacts with the upper face (the face that receives and donates the methyl group) of the corrinoid cofactor while the C-terminal domain of the CfsA provides the α-helix interacting on the lower face, the so called 'cap-helix'.

The homology detected between CfsA and HgcA occurs only with the C-terminal domain of CfsA and the N-terminal region of HgcA. This HgcA domain is predicted to bind the corrinoid in a 'base-off' state and has a cap-helix in the appropriate position to interact with the corrinoid. HgcA has a second domain containing predicted transmembrane regions at its C-terminus that has no homology to any features of $CFeSP_{Ch}$. The interaction of CfsA and CfsB

subunits of $CFeSP_{Ch}$ on either side of the corrinoid has been proposed to stabilize the Co(I) state of the cofactor. For catalytic function of $CFeSP_{Ch}$, the Cob(I)amide cofactor receives a methyl group as a carbocation from methyltetrahydrofolate via a methyltransferase (MeTr) to produce methylcob(III)amide. Similar catalytic features have been suggested for HgcA (Zhou et al. 2014). However, subsequent transfer of the methyl group from HgcA to Hg(II) as a carbanion would formally oxidize the cobalt of the cofactor to Co(III) . For continued catalytic function, the Co(III) corrinoid would need to be reduced by two electrons to Co(I) corrinoid, a reaction apparently not mediated by reductive activators of corrinoid enzymes (RACE proteins)(19, 20) but possibly mediated by the ferredoxin-like HgcB.

As stated, HgcA contains an apparently soluble domain proposed to include the site of the methylation reaction and a transmembrane domain of currently unknown function. Of possibly critical importance for the methylation of the presumed positively charged mercuric ion is the cysteine (Cys93) in the lower axial position of the cap-helix of HgcA, corresponding to the threonine (Thr374) in the $CFeSP_{Ch}$ used for modeling. This Cys93 in HgcA is unique among corrinoid proteins, as the vast majority of CFeSPs have an amino acid residue other than cysteine at this position facilitating displacement of the dimethylbenzimidazole ligand from cobalt (21, 22). This cysteine is highly conserved among all HgcA proteins identified in Hg(II) methylators (11)(Fig.1). The hypothesized transfer of a methyl carbanion to Hg(II) from methylcobalamin (Zhou et.al. 2014) may be facilitated by a Cys93 cysteine thiolate coordination to the Co(III) (23).

In addition to the two motifs for FeS centers in HgcB, this ferredoxin-like protein has two highly conserved vicinal cysteines at the extreme C-terminus that could serve any of several different roles, such as the reduction of HgcA, the delivery of Hg(II) to HgcA, the maintenance of structure or allow protein-protein interactions, or have no specific biochemical function. There is another conserved single cysteine (Cys73) in HgcB, also not part of either FeS center, that could possibly be involved in redox chemistry or even Hg(II) binding. Our initial mutant analysis of these residues provides evidence that several of these cysteines are critical for mercury methylation. Also expected to be necessary for the methylation process are proteins for transferring a methyl group to HgcA and for cofactor loading into HgcA. However, genes with those functions are apparently not unique to the genomes of methylating microbes.

We chose the known methylator ND132 (ND132) (24) to examine the conserved residues and apparent structural predictions for HgcA and HgcB since ND132 has been shown to be genetically accessible and a deletion mutant lacking *hcgAB* has been generated (11). Results from mutations in key regions of HgcA and HgcB that affect Hg(II) methylation are reported and discussed.

As yet there is no crystal structure of HgcA. The hypothesized corrinoid binding domain structure is from a threading experiment based on the crystal structure of *C. hydrogenoformans* Z-2901 CFeSP with the protein sequence deduced from the *hgcA* gene of ND132 (11). While we can state definitively that the mutations we have introduced have altered the functions of Hg(II) methylation, future studies will be needed to determine whether these mutations alter the catalytic capacity only, or also compromise the structure of the protein.

Materials and Methods

Reagents and Chemicals

All chemicals used were analytical grade and from either Sigma (St. Louis, MO) or Fisher Scientific (Pittsburgh, PA) unless otherwise stated.

Bacteria, culture media, growth conditions and antibiotics

All bacteria and plasmids used in this work are listed in supplemental Tables S1 and S2. Media compositions, cell growth, mercury exposure for methylation assays and DNA manipulations for mutagenesis were performed as previously described (11). For standard culturing or for methylation assays our basal salts medium with 0.1% (wt/vol) yeast extract (MOY salts; Zane et al., 2010) contained 60 mM lactate and 40 mM sulfate (MOYLS4) or 40 mM pyruvate and 40 mM fumarate (MOYPF) as carbon and electron sources, respectively. ND132 and *Desulfovibrio vulgaris* Hildenborough (ATCC 29579) (DvH) were always cultured anaerobically. *Escherichia coli* was grown aerobically for cloning purposes (25) or anaerobically for Hg(II) exposure experiments. Antibiotic resistance genes employed for selection were the following: kanamycin (Kn^R, *npt*), spectinomycin (Sp^R, *aadA*) and ampicillin (Ap^R, *bla*). For selection in *E. coli* all antibiotics were used at a concentration of 100 μg/ml; whereas, ND132 was determined to be sensitive to Kn, Sp and Ap at 400 μg/ml, 200 μg/ml, 100 μg/ml, respectively. Kn^R and Sp^R DvH were selected with 400 μg G418 (a kanamycin analog) and 200 μg spectinomycin/ml.

Site-directed mutation construction

All primers utilized and constructed for this study are listed in supplemental Table S3. For site-directed mutations in *hgcA* and *hgcB,* all plasmids were constructed to ensure that correct reading frame was conserved when integrated into the ND132 chromosome. Plasmid pMO4661 (Fig. 2; Table S1) was used as a template for all *hgcA* and *hgcB* mutations. This plasmid, a suicide (non-replicating) plasmid in ND132, includes, 5'-3', a 731-bp DNA region upstream of the predicted GTG start codon of *hgcA, hgcA* and *hgcB* ,a gene conferring Sp^R , and 762-bp DNA region downstream of *hgcB* TAG stop codon followed by an Ap^R gene and a pUC origin of replication. Three PCR amplicons were generated from pMO4661 to amplify the plasmid in three separate pieces (green primers and red primers in Fig. 2). Point mutations in *hgcA* or *hgcB* were introduced via PCR with primers designed to change the amino acid codons desired (red primers Fig. 2). With the three pieces reassembled in *E.coli* by SLIC (26), the new plasmid contained the desired point mutation that was confirmed by sequencing both strands containing the introduced mutation(s) and the homologous flanking regions. Selection in *E.coli* was with Sp^R and Ap^R. When this suicide plasmid was introduced into JWN1001, the ND132 *hgcAB* deletion strain containing Kn^R in place of the two genes, selection for Sp^R acquisition allowed the identification of double homologous recombination events where the Kn^R cassette of JWN1001 was replaced with the mutated *hgcA* or *hgcB* and the Sp^R marker. The resultant ND132 recombinant cells were screened for Sp^R and Ap^S.

HgcA *truncations*

For the C-terminal truncation of HgcA, once again pMO4661 was used as the template. Primers were designed to either delete the C-terminal domain of HgcA after amino acid 166

(Fig. 3A) or to mutate GAA of Glu187 to the non-sense mutation TAA STOP-187 (Fig. 3B). Mutant constructs were verified by sequencing on both strands.

ND132 electroporations

Electroporations and selection of recombinant ND132 colonies were performed as previously described (11).

Heterologous expression of hgcA *and* hgcB *in DvH and* E. coli.

To determine whether *hgcA* and *hgcB* provide the only gene functions required for Hg(II) methylation, the two genes were introduced into the non-methylating strains DvH and *E. coli* Silver cells. The parent strains and their derivatives, DvH(pMO4602) and *E. coli* Silver(pMO4602), harboring the stable plasmid pMO4602 heterologously expressing ND132 *hgcA* and *hgcB* were tested for their capacity to methylate Hg(II). Heterologous expression of *hgcA* and *hgcB* was verified by RT-PCR as previously described (11). DvH and *E.coli* derivatives containing *hgcA* and *hgcB* genes were grown anaerobically to an OD_{600} of ~0.7 at 34°C in MOYLS4 (DvH) or MOYPF supplemented with glucose (1 mM final concentration) (*E.coli*), respectively. Cells were then pelleted and resuspended in 1ml TRI-reagent (Gibco BRL, Life Technologies, Grand Island, NY) and stored at -80°C until RNA isolation and RT-PCR analysis.

Alignment of HgcA and HgcB from ND132 and D. alkaliphilus

Sequence alignments were performed by T-Coffee (27) and color converted for publication with BoxShade (http://www.ch.embnet.org/software/BOX_form.html).

Determination of the Hg-methylation potential by measurement of MeHg.

All exposures of bacteria to mercury were performed in a chamber (Coy Laboratory Products, Grass Lake, MI) containing a N_2:H_2 (95:5) anaerobic atmosphere and less than 0.5% O_2 (vol/vol). Deletion mutants for ND132 were sub-cultured into fresh medium as above (1% vol/vol) and grown until the OD_{600} reached ~0.5. These cultures were then diluted to an OD_{600} ~0.200 in fresh medium. The Hg(II) exposure was performed in triplicate in 2-ml microcentrifuge tubes containing 400 µl of culture to which $HgCl_2$ was added (10 ng/ml final concentration). These tubes were incubated in the dark for 2 h at 34°C. The cells were then immediately acidified with HNO_3 (3 N final concentration) and digested at room temperature for 24 h before analysis. Wild-type ND132 was used as a positive mercury methylation control. Non-methylating controls were: heat-killed ND132; viable Δ*hgcAB* mutant strain, JWN1001 (11); and sterile medium as an abiotic control. Mutants were also tested as heat-killed cultures. None of the non-methylating controls, JWN1001 or abiotic medium showed methylmercury production levels above either ND132 heat killed control or the detection limits (see below).

Methylmercury production was determined by Ethylation Purge and Trap Gas Chromatography Atomic Fluorescence Spectrometry (EPT-GC-AFS) according to EPA method 1630 (*nepis.**epa**.gov/Exe/ZyPURL.cgi?Dockey=P100IKBQ.TXT*). All manipulations were performed at room temperature in a fume hood. An aliquot (80 µl) of the acidified sample was added to 40 ml sodium acetate buffer (1 M acetic acid, 1 M sodium acetate, pH 3.9). Hg species were then ethylated with 50 µl sodium tetraethylborate (1% wt/vol) and extracted from the solution into an automated purge and trap system followed by gas chromatographic separation and quantification by AFS with a MERX Hg speciation GC and Pyrolysis Module coupled to a Model III Cold Vapor Atomic Fluorescence Spectrophotometer. Data were integrated with

Mercury Guru 4.1 software and peaks were quantified by comparison with a MeHg standard curve. Mercury chloride ($HgCl_2$) and methylmercury chloride (CH_3HgCl) were used for Hg-methylation assays and external calibration, respectively, and were all greater than 95% pure. The experimental detection limits determined with analytical blanks (n=15) for each experimental batch were ≤ 0.52±0.1 pg/ml. All equipment, reagents, standards and software for MeHg detection were from Brooks Rand Labs, Seattle, WA.

Antibody development and western blot analysis

A rabbit polyclonal antibody to amino acids 18-29 of HgcA (epitope YLRRDDRVGDLR) was developed and affinity purified by Anaspec (Fremont, CA). Western analysis, including SDS-PAGE, protein transfer to membrane, and immunoblotting generally followed the procedures of Shapiro et al.; Towbin et al.; and Burnett (28-30) with details and modifications described as follows. ND132 cultures grown in 200 ml MOYPF at on OD_{600} of 0.5 were centrifuged at 4000 x *g* for 12 min at 4°C. The cell pellet was resuspended, washed, and centrifuged again in 50 ml of cold 50 mM potassium phosphate (KPi) buffer (pH 7.2) with 10 mM dithiothreitol (DTT). The cell pellet was then resuspended in 10 ml of 50 mM cold KPi buffer with 10 mM DTT, 1 mM phenylmethylsulfonyl fluoride (PMSF), and 100 µl bacterial protease inhibitor cocktail (Sigma, St. Louis, MO). The cell suspension was passed through a French press twice at 19000 psi. The lysate was then centrifuged at 4000 x *g* for 12 min and the supernatant was recovered. This supernatant was then spun at 17000 x *g* for 15 min at 4°C and the resulting supernatant was saved for protein analysis. Protein concentrations were determined by the Bradford method (31) with BSA as a standard. Precast 12% (wt/vol) TGX gels (Bio-Rad, Hercules, CA) were used

to separate cellular proteins. Protein extracts were loaded onto the gels at 30 µg per lane in denaturing Laemmli loading buffer(32). Gels were run for 90 min at 100 V at room temperature (RT) in Tris-Glycine SDS buffer consisting of 25 mM Tris pH 8.3, 0.2 M glycine, and 3.5 mM SDS on the Mini-PROTEAN system (Bio-Rad). Protein transfer to PVDF membrane (Millipore, Billerica, MA) was performed overnight at 150 mA in 4°C in transfer buffer containing 25 mM Tris pH 8.3, 192 mM glycine, and 20% (vol/vol) methanol. After transfer, membranes were washed briefly with Tris-buffered saline (20 mM Tris and 150 mM NaCl, pH 7.5) with 0.2% (vol/vol) Tween 20 (TBST). Membranes were then blocked for 1 h in TBST+ 5% (vol/vol) goat serum (MP Biomedicals, Santa Ana, CA) at RT. After blocking, membranes were incubated with primary rabbit anti-HgcA at a dilution of 1:5000 in TBST+5% (vol/vol) goat serum for 1 h at RT. Membranes were then washed 3 times for 5 min each in TBST and subsequently incubated for 1 h at RT with secondary goat anti-rabbit IgG-HRP (Sigma) conjugated antibody at a 1:3000 dilution in TBST+5% (vol/vol) goat serum. After secondary antibody incubation membranes were washed three times for 5 min each in TBST. Chemiluminescence detection was performed with Pierce© ECL western blotting substrate (Thermo Scientific, Rockford, IL) per manufacturer instructions. Membranes were exposed to X-ray film (Thermo Scientific) for three to 45 s and developed in an X-ray film processor (SRX-101A, Kinoca Minolta, China). Denatured protein migration positions were compared to protein standards (Bio-Rad) to verify molecular weight. JWN1001, the Δ*hgcAB* strain, served as a negative control for HgcA.

Results

The prediction and subsequent confirmation of the enzymes essential for Hg(II) methylation led to the development of a novel model for the mechanism of methyl transfer by the corrinoid HgcA. Although the nature of the actual Hg(II) substrate is not known, it was reasoned that a methyl carbanion might more readily interact if the mercury carried a positive charge, and theoretical calculations have supported the prediction (23). The observation of the conserved cysteine in the cap helix was suggested to provide a lower axial ligand to the cobalt of the corrinoid cofactor as a thiolate to stabilize the cobamide during the transfer of the methyl carbanion.

We first tested the necessity of the conserved Cys93 and the cap helix region hypothesized to be integral to the methylation reaction (11, 23). When we mutated Cys93 of the cap helix region of HgcA to either Thr93, found in the corresponding position in $CFeSP_{Ch,}$ or Ala93, MeHg production was eliminated (Fig. 4, Table 1). When Cys93 was mutated to His93, commonly found in other corrinoid proteins, MeHg was detected, however, at only 5% of that produced by wild type ND132. When Trp92, which resides just proximal to Cys93 (Fig.1), was changed to Ala92 we saw a reduction of MeHg produced to 30% of wild-type levels. When the aromatic side chain Trp92 was replaced with another aromatic side chain, Phe92, methylation was decreased to 5-10% of wild type. These results show the importance of the Cys93 and its neighboring amino acid, Trp92, in the methylation reaction.

To determine the contribution of the cap helix region toward Hg(II) methylation, we systematically disrupted the region through alanine scanning. This approach has been shown to provide insights into the influence of amino acid side chain chemistry on protein reactivity

(33). After systematically mutating individual amino acid residues around the cap helix Cys93 to alanine, other than the adjacent Trp92, the confirmed site-directed mutants were found not to change the Hg(II) methylation capacity from that of wild type ND132 (Fig. 4; Table 1). Residues 94 and 95 are Ala in wild-type HgcA, so these were mutated separately to Ser94 or Ser95, and the mutants also showed no difference in MeHg production from that of wild-type. (Fig. 4; Table 1) A proven technique to disrupt protein helical structure is to convert a residue within the helix to a proline (34, 35). Site-directed proline mutations designed to disrupt the cap helix region of HgcA near Cys93 were introduced singly into HgcA. The mutations Val91Pro, Trp92Pro, Ala94Pro, Ala95Pro and Gly98Pro all led to decreases in methylation capacity (Fig. 4; Table 1). These results supported the prediction of a helical structure for the region where Cys93 is located. These observations strengthen the hypotheses that the helix plays a role in positioning Cys93 for liganding with the cobalt in the corrinoid cofactor and that the cap-helix stabilizes the Co(I) redox state. With the exception of Cys93, evidence is also provided that the cap helix amino acid residue chemistry is less important than maintenance of structure.

In order determine if the N-terminal domain of HgcA could retain biochemical activity in the absence of the transmembrane domain, we truncated the protein with two separate approaches. We first removed the coding sequence of the C-terminal domain of HgcA from amino acid 167 through the end of the protein. The resulting mutant with this truncation was unable to methylate Hg(II) (Table 1). Through preliminary experiments to determine the transcriptional start sites (TSS) of *hgcA* and *hgcB* (data not shown), we observed that the C-terminal region of *hgcA* harbors a TSS of *hgcB* 144 bp upstream of the ATG start codon of *hgcB*. If the primary TSS of *hgcB* were indeed located in the 3'-terminal region of *hgcA*, HgcB would

not be expressed when that DNA was deleted, and its absence would provide an established reason for the lack of methylation activity. Therefore, we engineered a translational stop site just after the N-terminal domain of HgcA, replacing amino acid 187 (codon GAA) with a TAA stop site, 329 bp upstream of the putative TSS of *hgcB*. This stop codon produces a 186 amino acid N-terminal HgcA fragment but does not eliminate the TSS for transcription of *hgcB*. When this mutation was successfully introduced, mercury methylation by the mutant strain was still not detected (Table 1). We interpreted these results to suggest that the apparent transmembrane domain of HgcA was needed for the methylation function.

Verification of expression of the soluble domain of HgcA in the context of the above non-sense mutant was attempted by western blot analysis with the antibody directed against amino acids 18-29 of HgcA. Western blot analysis showed a band corresponding to full length HgcA at ~40 kD in wild-type ND132 controls, but, in the mutant strain, there was no evidence of the truncated ~20 kD form of HgcA (Fig. 5). Therefore the absence of mercury methylation could result from an absence of the transmembrane domain of HgcA or from rapid turn-over of this truncated N-terminal domain.

HgcB, predicted to be a ferredoxin, has two highly conserved vicinal cysteines at the extreme C-terminus (11). Vicinal cysteines in proteins have been shown to have the potential for binding Hg(II) (36) or to possibly function as a redox switch in proteins (37, 38). To examine the impact of mutations in the conserved vicinal cysteines in HgcB of ND132, each cysteine was mutated individually to alanine, and then a double mutant was constructed in which both were converted to alanines. When these mutants were tested for their mercury methylation

capacity, the Cys95Ala or Cys96Ala mutants of HgcB separately showed no change in methylation levels from wild type ND132, but mutating both in the same protein led to reduction of methylation to 10% of wild type ND132 (Table 1). Apparently only one cysteine is needed in the C-terminus of HgcB for full function. This result also would indicate that binding of Hg(II) by the vicinal cysteines together does not significantly contribute to the methylation function. However, another cysteine was present in HgcB (and conserved in many of the HgcB proteins sequenced) that was not part of an FeS center, Cys73, which could undergo dithiol oxidation/reduction reactions with either of the viscinal cysteines. When mutated to alanine, HgcB with Cys73Ala showed no methylation.

Discussion

To examine the function of conserved amino acids and protein regions of HgcA and HgcB, proteins necessary for Hg(II) methylation, and to test predicted features of the putative structure of HgcA, site-directed mutations and specific deletions in the encoding genes were made. This approach was facilitated by having a mutant of *D. desulfuricans* ND132 deleted for both genes replaced by a selectable marker (11). Importantly, the first feature examined was the unusual chemistry predicted for the corrinoid protein HgcA. This protein was suggested to transfer a methyl carbanion to mercury, chemistry not yet demonstrated for biological methyl transfer by a cobamide enzyme. Typical corrinoid methyltransferase chemistry described in past literature has generally involved transfer of a methyl carbocation (39). The transfer of a carbanion by HgcA (11, 23) would likely be facilitated by a cysteine thiolate (Cys93) positioned

in the cap-helix that could coordinate the cobalt of the corrinoid cofactor during the methyl transfer. For this reason we targeted Cys93 in the cap helix for mutagenesis. The elimination of methylation capacity in strains harboring mutations of HgcA Cys93 was interpreted as supporting the hypothesis that this residue is indeed functioning to facilitate carbanion transfer.

It is interesting that Cys93, when mutated to His93, retains a small percentage of methylating capacity. In many corrinoid proteins, the cap-helix residue in closest proximity to the Co of the corrinoid is indeed a histidine (21). Using density functional theory calculations, Zhou et al. (23)suggested that histidine ligand exchange during carbanion transfer to Hg(II) should also facilitate transfer of the methyl carbanion.

As shown in the weighted amino acid logo of the cap helix region (Fig. 1), certain amino acids in the cap helix are more conserved than others with Trp92 being one of the most highly conserved. The fact that Trp92, a bulky, aromatic amino acid, when changed to Ala92 resulted in a 70% reduction of methylation capacity suggests that this residue, adjacent to Cys93, is functionally important. Additional structural studies will be needed to differentiate between possible roles of the Trp residue, for example, positioning Cys93 for access to the corrinoid cofactor or for providing protection to the Co(I) through hydrophobic interactions with the corrinoid ring. Mutation of the other amino acids of the cap-helix through alanine scanning or by introduction of a helix-disrupting proline showed that structure of this region was critical for the methylation, supporting inferences from the structural homology with $CFeSP_{Ch}$.

The exact structure of the corrinoid derivative involved in the mercury methylation reaction is not known, but clearly the electronic state of the Co will be affected by the side chains of the ring as will the ligand exchange reactions involved in the methyl transfer. With unusual chemistry predicted for HgcA, a modified corrinoid may be present. DvH has been shown to date to be the only organism to synthesize rare guanylcobamide and hypoxanthylcobamide corrinoids and not to produce pseudovitamin B_{12} (40). The nature of the side chain of the cobamide involved in the Hg(II) methylation reaction may help confer the ability to methylate Hg(II). The specific corrinoid(s) synthesized by ND132 has not yet been determined.

Completing the methyl transfer to Hg(II) results in the formal oxidation of the cobalt, generating Cob(III)amide in HgcA. For the cycle to continue, two electrons are needed to reduce the Co(III) to Co(I) to ready HgcA to accept another CH_3^+ carbocation (Fig. 6). The ferredoxin, encoded by the gene *hgcB* immediately downstream of *hgcA* and essential for methylation of mercury, is the logical donor for reducing Co(III) to Co(I), as was hypothesized (11, 23). Because Cys95 and Cys96 at the C-terminus of HgcB were found to be highly conserved among the homologs in methylators, we targeted these residues for site-directed mutagenesis and found that one of the two would appear to be needed. It is known that vicinal cysteines poorly mediate redox reactions because of the strained stereochemistry between the two cysteines (35) but they have been shown to act as conformational redox switches (38). Of note, another cysteine (Cys73) in HgcB, that is not part of either FeS center, when mutated to alanine showed no Hg(II) methylation. Future studies may determine whether Cys73 functions in conjunction with either of the vicinal cysteines for electron movement and/or provides needed structural features.

In all but one of the HgcB homologs in Hg(II) methylating microorganisms found to date, vicinal cysteines are present in the C-terminal region of the protein along with a cysteine residue analogous to the Cys73 of HgcB in strain ND132. The single Hg(II) methylating bacterium that does not follow this rule is *Dethiobacter alkaliphilus* strain AHT 1 (DSM 19026, *Dt. alkaliphilus*) (18, 41) that is truncated after Gly71, which corresponds to Gly72 in ND132, just upstream of the expected position of Cys73 (Fig. 7A). It was observed that HgcA of *Dt. alkaliphilus* has an insert in the extreme N-terminal region of 29 amino acids containing two pairs of vicinal cysteines separated by three amino acids (Fig.7B). It is tempting to speculate that these inserted cysteines of HgcA in *Dt. alkaliphilus* might functionally replace the vicinal cysteines lacking in HgcB. Future experiments reconstructing this arrangement of cysteines in the genetically accessible ND132 might allow testing of this hypothesis.

Our studies show that the putative transmembrane domain of HgcA is needed, at a minimum, for stability of the N-terminal corrinoid-binding region. The hydrophobic C-terminal region may protect the cofactor, localize the protein (42) or possibly facilitate Hg(II) transport into, or MeHg out of, the cell. Lin et al. (43) have shown that the *hgcAB* double deletion mutant of *Geobacter sulfurreducens* PCA has decreased Hg(II) uptake and metabolism by about 30%. The predicted transmembrane domain of HgcA has no homology to any other known transmembrane protein (11) making comparison of this region for suggested functions limited.

While this study sheds new light on the structural aspects of HgcA and HgcB required for maximal mercury methylation, many questions remain unanswered. It is predicted that these proteins normally carry out a different function in methylating bacteria but that unidentified

role is not essential under laboratory culture conditions. The mechanism of Hg(II) recognition, the sources of the methyl group found in the methylmercury, the methyl transferase donating the predicted carbocation to HgcA, and the sources of reductant for continued catalytic function require investigation. The identities of additional protein components of the reaction may contribute to our understanding of any alternative physiological function of HgcA and HgcB in anaerobic microbes.

Acknowledgments

This work was supported by the U.S. Department of Energy (DOE) Office of Science, Biological and Environmental Research, Subsurface Biogeochemical Research (SBR) Program through grants DE-FG02-07ER64396 and DE SC0006809 (to J.D.W.) and subcontract #40000099987 from the ORNL Science Focus Area on mercury. ORNL is managed by UT-Battelle, LLC for US DOE under contract DE-AC05-00OR22725.

References (mostly formatted for AEM)

1. **Wood JM.** 1974. Biological cycles for toxic elements in the environment. Science (New York, N.Y.) **183:**1049-1052.
2. **Hintelmann H.** 2010. Organomercurials. Their formation and pathways in the environment. Metal ions in life sciences **7:**365-401.
3. **Driscoll CT, Mason RP, Chan HM, Jacob DJ, Pirrone N.** 2013. Mercury as a global pollutant: sources, pathways, and effects. Environmental science & technology **47:**4967-4983.
4. **Lamborg CH, Hammerschmidt CR, Bowman KL, Swarr GJ, Munson KM, Ohnemus DC, Lam PJ, Heimburger L-E, Rijkenberg MJA, Saito MA.** 2014. A global ocean inventory of anthropogenic mercury based on water column measurements. Nature **512:**65-68.
5. **Harris RC, Rudd JW, Amyot M, Babiarz CL, Beaty KG, Blanchfield PJ, Bodaly RA, Branfireun BA, Gilmour CC, Graydon JA, Heyes A, Hintelmann H, Hurley JP, Kelly CA, Krabbenhoft DP, Lindberg SE, Mason RP, Paterson MJ, Podemski CL, Robinson A, Sandilands KA, Southworth GR, St Louis VL, Tate MT.** 2007. Whole-ecosystem study shows rapid fish-mercury response to changes in mercury deposition. Proceedings of the National Academy of Sciences of the United States of America **104:**16586-16591.
6. **Vazquez M, Velez D, Devesa V.** 2014. In Vitro Characterization of the Intestinal Absorption of Methylmercury using a Caco-2 Cell Model. Chemical research in toxicology **27:**254-264.
7. **Compeau GC, Bartha R.** 1985. Sulfate-reducing bacteria: principal methylators of mercury in anoxic estuarine sediment. Appl Environ Microbiol **50:**498-502.
8. **Gilmour CC, Henry EA, Mitchell R.** 1992. Sulfate stimulation of mercury methylation in freshwater sediments. Environ Sci Technol **26:**2281-2287.
9. **Yu RQ, Reinfelder JR, Hines ME, Barkay T.** 2013. Mercury methylation by the methanogen Methanospirillum hungatei. Appl Environ Microbiol **79:**6325-6330.
10. **Hamelin S, Amyot M, Barkay T, Wang Y, Planas D.** 2011. Methanogens: principal methylators of mercury in lake periphyton. Environmental science & technology **45:**7693-7700.
11. **Parks JM, Johs A, Podar M, Bridou R, Hurt RA, Jr., Smith SD, Tomanicek SJ, Qian Y, Brown SD, Brandt CC, Palumbo AV, Smith JC, Wall JD, Elias DA, Liang L.** 2013. The genetic basis for bacterial mercury methylation. Science (New York, N.Y.) **339:**1332-1335.
12. **Choi SC, Bartha R.** 1993. Cobalamin-mediated mercury methylation by Desulfovibrio desulfuricans LS. Appl Environ Microbiol **59:**290-295.
13. **Choi SC, Chase T, Jr., Bartha R.** 1994. Enzymatic catalysis of mercury methylation by Desulfovibrio desulfuricans LS. Appl Environ Microbiol **60:**1342-1346.
14. **Choi SC, Chase T, Bartha R.** 1994. Metabolic Pathways Leading to Mercury Methylation in Desulfovibrio desulfuricans LS. Appl Environ Microbiol **60:**4072-4077.
15. **Berman M, Chase T, Bartha R.** 1990. Carbon Flow in Mercury Biomethylation by Desulfovibrio desulfuricans. Appl Environ Microbiol **56:**298-300.
16. **Goetzl S, Jeoung JH, Hennig SE, Dobbek H.** 2011. Structural basis for electron and methyl-group transfer in a methyltransferase system operating in the reductive acetyl-CoA pathway. Journal of molecular biology **411:**96-109.
17. **Svetlitchnaia T, Svetlitchnyi V, Meyer O, Dobbek H.** 2006. Structural insights into methyltransfer reactions of a corrinoid iron-sulfur protein involved in acetyl-CoA synthesis. Proceedings of the National Academy of Sciences of the United States of America **103:**14331-14336.

18. **Gilmour CC, Podar M, Bullock AL, Graham AM, Brown SD, Somenahally AC, Johs A, Hurt RA, Jr., Bailey KL, Elias DA.** 2013. Mercury methylation by novel microorganisms from new environments. Environmental science & technology **47:**11810-11820.
19. **Kaufmann F, Wohlfarth G, Diekert G.** 1998. O-demethylase from Acetobacterium dehalogenans--substrate specificity and function of the participating proteins. European journal of biochemistry / FEBS **253:**706-711.
20. **Nguyen HD, Studenik S, Diekert G.** 2013. Corrinoid activation by a RACE protein: studies on the interaction of the proteins involved. FEMS microbiology letters **345:**31-38.
21. **Ludwig ML, Matthews RG.** 1997. Structure-based perspectives on B12-dependent enzymes. Annual review of biochemistry **66:**269-313.
22. **Hazra AB, Tran JL, Crofts TS, Taga ME.** 2013. Analysis of substrate specificity in CobT homologs reveals widespread preference for DMB, the lower axial ligand of vitamin B(12). Chemistry & biology **20:**1275-1285.
23. **Zhou J, Riccardi D, Beste A, Smith JC, Parks JM.** 2014. Mercury methylation by HgcA: theory supports carbanion transfer to Hg(II). Inorganic chemistry **53:**772-777.
24. **Gilmour CC, Elias DA, Kucken AM, Brown SD, Palumbo AV, Schadt CW, Wall JD.** 2011. Sulfate-reducing bacterium Desulfovibrio desulfuricans ND132 as a model for understanding bacterial mercury methylation. Appl Environ Microbiol **77:**3938-3951.
25. **Zane GM, Bill Yen HC, Wall JD.** 2010. Effect of the deletion of *qmoABC* and the promoter-distal gene encoding a hypothetical protein on sulfate reduction in *Desulfovibrio vulgaris* Hildenborough. Appl. Environ. Microbiol. **76:**5500-5509.
26. **Hill RE, Eaton-Rye JJ.** 2014. Plasmid construction by SLIC or sequence and ligation-independent cloning. Methods Mol Biol **1116:**25-36.
27. **Magis C, Taly JF, Bussotti G, Chang JM, Di Tommaso P, Erb I, Espinosa-Carrasco J, Notredame C.** 2014. T-Coffee: Tree-based consistency objective function for alignment evaluation. Methods Mol Biol **1079:**117-129.
28. **Shapiro AL, Vinuela E, Maizel JV, Jr.** 1967. Molecular weight estimation of polypeptide chains by electrophoresis in SDS-polyacrylamide gels. Biochem Biophys Res Commun **28:**815-820.
29. **Towbin H, Staehelin T, Gordon J.** 1992. Electrophoretic transfer of proteins from polyacrylamide gels to nitrocellulose sheets: procedure and some applications. 1979. Biotechnology (Reading, Mass.) **24:**145-149.
30. **Burnette WN.** 1981. "Western blotting": electrophoretic transfer of proteins from sodium dodecyl sulfate--polyacrylamide gels to unmodified nitrocellulose and radiographic detection with antibody and radioiodinated protein A. Analytical biochemistry **112:**195-203.
31. **Bradford MM.** 1976. A rapid and sensitive method for the quantitation of microgram quantities of protein utilizing the principle of protein-dye binding. Anal. Biochem. **72:**248-254.
32. **Laemmli UK.** 1970. Cleavage of structural proteins during the assembly of the head of bacteriophage T4. Nature **227:**680-685.
33. **Morrison KL, Weiss GA.** 2001. Combinatorial alanine-scanning. Current opinion in chemical biology **5:**302-307.
34. **von Heijne G.** 1991. Proline kinks in transmembrane alpha-helices. Journal of molecular biology **218:**499-503.
35. **Nilsson I, Saaf A, Whitley P, Gafvelin G, Waller C, von Heijne G.** 1998. Proline-induced disruption of a transmembrane alpha-helix in its natural environment. Journal of molecular biology **284:**1165-1175.
36. **DeSilva TM, Veglia G, Porcelli F, Prantner AM, Opella SJ.** 2002. Selectivity in heavy metal-binding to peptides and proteins. Biopolymers **64:**189-197.

37. **Carugo O, Cemazar M, Zahariev S, Hudaky I, Gaspari Z, Perczel A, Pongor S.** 2003. Vicinal disulfide turns. Protein engineering **16:**637-639.
38. **Wouters MA, Fan SW, Haworth NL.** 2010. Disulfides as redox switches: from molecular mechanisms to functional significance. Antioxidants & redox signaling **12:**53-91.
39. **Matthews RG.** 2009. Cobalamin-and corrinoid-dependent enzymes. Metal ions in life sciences **6:**53.
40. **Guimarães DH, Weber A, Klaiber I, Vogler B, Renz P.** 1994. Guanylcobamide and hypoxanthylcobamide-Corrinoids formed by Desulfovibrio vulgaris. Archives of microbiology **162:**272-276.
41. **Sorokin DY, Tourova TP, Mussmann M, Muyzer G.** 2008. Dethiobacter alkaliphilus gen. nov. sp. nov., and Desulfurivibrio alkaliphilus gen. nov. sp. nov.: two novel representatives of reductive sulfur cycle from soda lakes. Extremophiles : life under extreme conditions **12:**431-439.
42. **Hagerhall C, Hederstedt L.** 1996. A structural model for the membrane-integral domain of succinate: quinone oxidoreductases. FEBS letters **389:**25-31.
43. **Lin H, Hurt Jr R, Johs A, Parks JM, Morrell-Falvey JL, Liang L, Elias D, Gu B.** 2014. Unexpected effects of gene deletion on mercury interactions with the methylation-deficient mutant ΔhgcAB. Environmental Science & Technology Letters.
44. **Thomsen MC, Nielsen M.** 2012. Seq2Logo: a method for construction and visualization of amino acid binding motifs and sequence profiles including sequence weighting, pseudo counts and two-sided representation of amino acid enrichment and depletion. Nucleic acids research **40:**W281-287.

Figure legends

Fig. 1. Weighted amino acid analysis of the cap-helix and amino acid region surrounding Cys93 of HgcA (numbering from ND132) from sequences of 20 tested bacteria known to methylate mercury. The size of the letter for the amino acid correlates with the level of conservation (44). All amino acids below the x-axis were not identified in that stretch of sequence in the 20 Hg(II) methylating organisms selected from (11, 18). Created by Seq2Logo (http://www.cbs.dtu.dk/biotools/Seq2Logo/) (44).

Fig. 2. Diagram of the mutational strategy for creating point mutations in *hgcA* (purple) of pMO4661 (Fig. 2A.) In this example (Fig. 2B.) the red primers were designed to mutate Cys93 while the blue primers were to amplify sections of the plasmid backbone. An enlarged diagram (Fig. 2C) of *hgcAB* showing the location of the cysteine residue in the cap helix that was mutated by this site-directed mutation procedure. PCR amplicons assembly was by the SLIC procedure (Li and Elledge, 2007).

Fig. 3. Primer design for removing the C-terminal transmembrane domain of *hgcA*. Fig. 3A, Genetic deletion strategy. Rectangles represent the genes and DNA features in the *hgcAB* region of the chromosome. Arrows are primers. Identical primer color reflects complementary sequences. The red color in the primers indicates that the STOP codon of *hgcA* was retained. Yellow represents the 14bp intergenic region between *hgcA* and *hgcB* in ND132. Fig. 3B,

construct showing deletion of the DNA encoding the C-terminal region of HgcA. Fig 3C, construct showing the position of the mutation of Gly187 to STOP-187, retaining the downstream coding region of HgcA which harbors the putative TSS of HgcB.

Fig. 4. Alteration of the Hg(II) methylation potential by amino-acid (a.a.) substitutions centered toward the chemically important cysteine Cys93 (identified by the blue arrow) in the predicted cap helix of the cobalamin binding domain of HgcA in *D. desulfuricans* ND132. MeHg production (%) of the mutants as compared to the *D. desulfuricans* ND132 wild type control; also depicted across the putative cap helix with (red) as completely altered, (orange) as intermediate and (green) unaltered. Evidence for the helical structure of this peptide was provided by proline (P) substitutions; whereas the chemical importance of the a.a. residues was tested by substitution to an alanine (A) or a serine (S). Other a.a. substitutions to either phenylalanine (F), threonine (T) or histidine (H) were relevant regarding computational quantum chemistry predictions (Zhou et al., 2013) or based on orthologous CFeSP a.a. frequency from methylating and non-methylating organisms (Parks et al., 2013).

Fig. 5. Western blot showing expression of full length HgcA from wild type ND132 (lane 1) and no detection of truncated HgcA in the non-sense mutant (lane 3). Lane 2 is JWN1001, the Δ*hgcAB* strain used as a negative control. Note the non-specific band above HgcA in all three samples showing equal loading of samples.

Fig. 6. The methylation reaction carried out by HgcA and HgcB, showing the THF-methyltransferase (labeled MeTr), from the reductive acetyl CoA pathway, providing the methyl group that eventually becomes bound to Hg. From Parks et al. (11).

Fig. 7. Alignments of HgcB and HgcA of ND132 compared to *Dt. alkaliphilus*. Strictly conserved amino acids are in black, while chemically similar amino acids are in gray. Fig. 7A. Alignment of HgcB of ND132 and *Dt. alkaliphilus* showing the locations of Cys73 and the vicinal cysteines of $HgcB_{ND132}$ (red), and $HgcB_{Dt.\ alkaliphilus}$ illustrating the truncation at Gly71 (what would be Gly72 in ND132) and lack of Cys73 and the vicinal cysteines. The cysteines of the two FeS clusters ($CX_2CX_2CX_3C$) are shown in yellow. Fig. 7B. Alignment of HgcA of ND132 and *Dt. alkaliphilus* showing full length $HgcA_{ND132}$ and $HgcA_{Dt.\ alkaliphilus}$ showing the 29 amino acid insert 84 amino acids upstream of the cap helix (yellow), and the two pairs of vicinal cysteines (red) in the insert.

Fig. 1

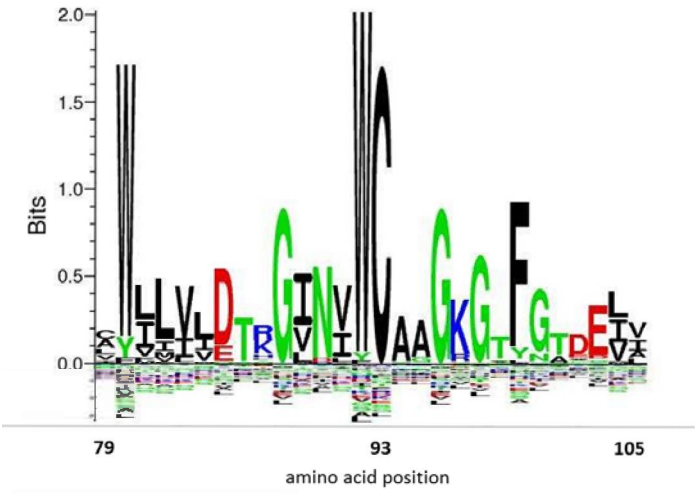

Fig. 2

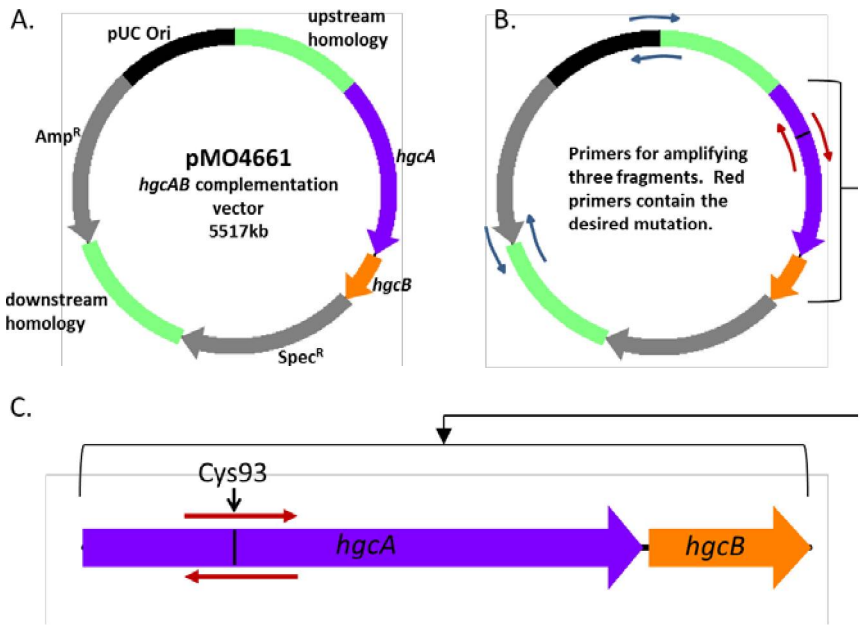
A.
pUC Ori
upstream homology
Amp^R
pMO4661
hgcAB complementation vector
5517kb
hgcA
hgcB
downstream homology
Spec^R
B.
Primers for amplifying three fragments. Red primers contain the desired mutation.
C.
Cys93
hgcA
hgcB

Fig. 3

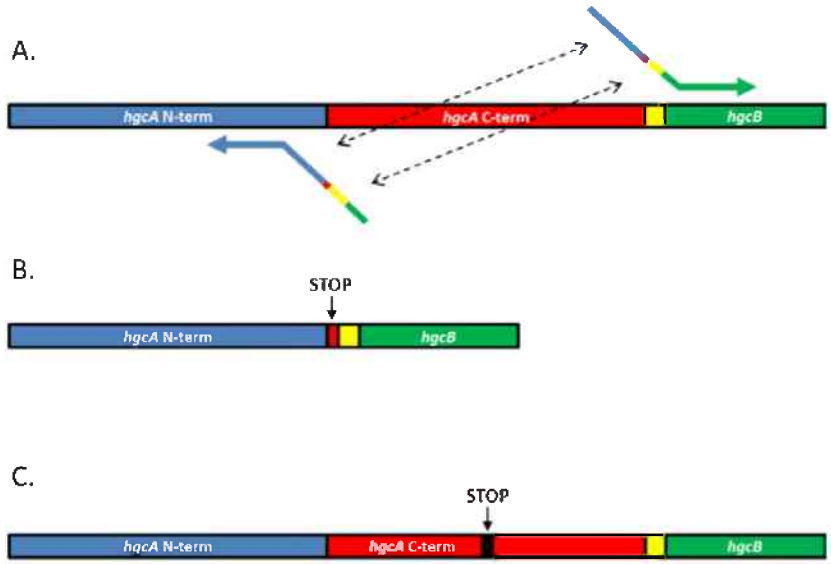
A.
hgcA N-term
hgcA C-term
hgcB
B.
STOP
hgcA N-term
hgcB
C.
STOP
hgcA N-term
hgcA C-term
hgcB

Fig. 4


HgcA
putative cobalamin-binding domain
predicted transmembrane domain
Desulfovibrio desulfuricans ND132
[a]MeHg (%)
predicted cap helix
Desulfovibrio desulfuricans ND132_Mutants
JWN1022 hgcA codon 87 (R87A) AWL LVVDTGI NV WC AA GKGLF TASEVA 100
JWN1021 hgcA codon 88 (G88A) AWL LVVDTRI NV WC AA GKGLF TASEVA 100
JWN1020 hgcA codon 89 (I89A) AWL LVVDTRG NV WC AA GKGLF TASEVA 100
JWN1019 hgcA codon 90 (N90A) AWL LVVDTRGI V WC AA GKGLF TASEVA 100
JWN1064 hgcA codon 90 (N90P) AWL LVVDTRGI V WC AA GKGLF TASEVA 40
JWN1018 hgcA codon 91 (V91A) AWL LVVDTRGI N WC AA GKGLF TASEVA 100
JWN1065 hgcA codon 91 (V91P) AWL LVVDTRGI N WC AA GKGLF TASEVA 8
JWN1017 hgcA codon 92 (W92A) AWL LVVDTRGI NV C AA GKGLF TASEVA 30
JWN1068 hgcA codon 92 (W92P) AWL LVVDTRGI NV C AA GKGLF TASEVA 0
JWN1069 hgcA codon 92 (W92F) AWL LVVDTRGI NV C AA GKGLF TASEVA 5
JWN1016 hgcA codon 93 (C93A) AWL LVVDTRGI NV W AA GKGLF TASEVA 0
JWN1006 hgcA codon 93 (C93T) AWL LVVDTRGI NV W AA GKGLF TASEVA 0
JWN1045 hgcA codon 93 (C93H) AWL LVVDTRGI NV W AA GKGLF TASEVA 5
JWN1029 hgcA codon 94 (A94S) AWL LVVDTRGI NV WC A GKGLF TASEVA 100
JWN1066 hgcA codon 94 (A94P) AWL LVVDTRGI NV WC A GKGLF TASEVA 0
JWN1030 hgcA codon 95 (A95S) AWL LVVDTRGI NV WC A GKGLF TASEVA 100
JWN1067 hgcA codon 95 (A95P) AWL LVVDTRGI NV WC A GKGLF TASEVA 0
JWN1023 hgcA codon 96 (G96A) AWL LVVDTRGI NV WC AA KGLF TASEVA 100
JWN1024 hgcA codon 97 (K97A) AWL LVVDTRGI NV WC AA G GLF TASEVA 100
JWN1025 hgcA codon 98 (G98A) AWL LVVDTRGI NV WC AA GK LF TASEVA 100
JWN1073 hgcA codon 98 (G98P) AWL LVVDTRGI NV WC AA GK LF TASEVA 50
JWN1026 hgcA codon 99 (L99A) AWL LVVDTRGI NV WC AA GKG F TASEVA 100
JWN1027 hgcA codon 100 (F100A) AWL LVVDTRGI NV WC AA GKGL TASEVA 100
JWN1028 hgcA codon 101 (T101A) AWL LVVDTRGI NV WC AA GKGLF ASEVA 100

Fig 5.

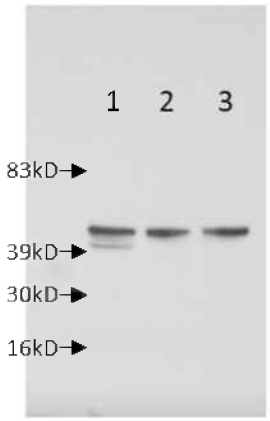

Fig. 6

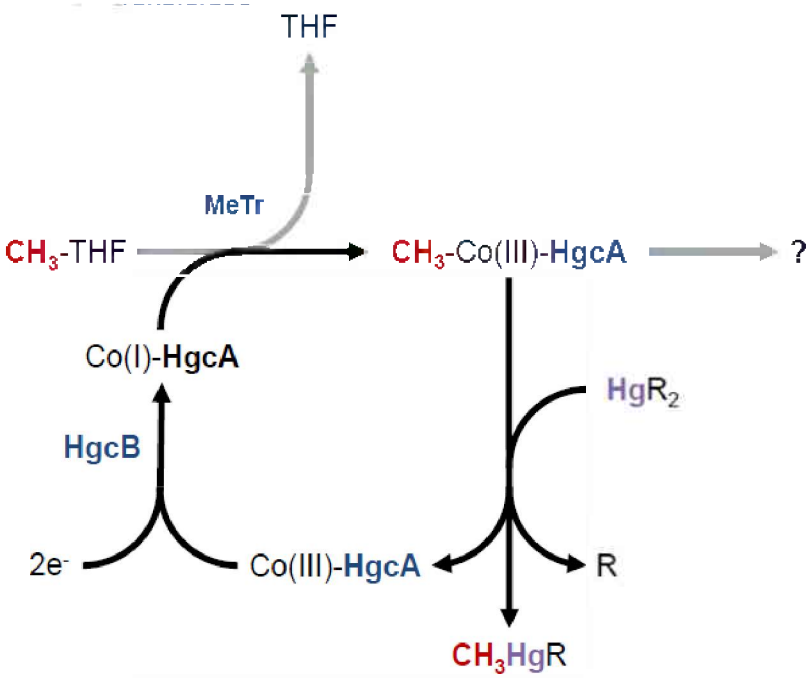
THF
MeTr
CH3-THF
CH3-Co(III)-HgcA
?
Co(I)-HgcA
HgR2
HgcB
2e-
Co(III)-HgcA
R
CH3HgR

Fig. 7A.

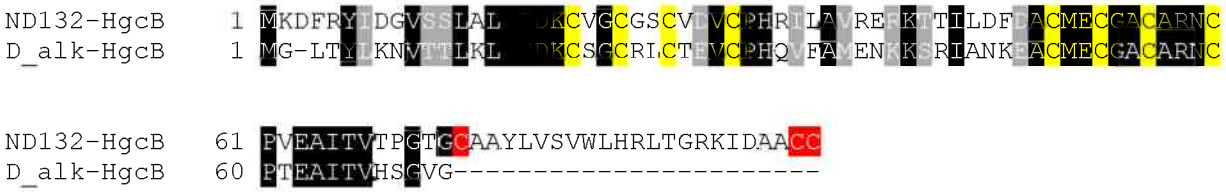

Fig. 7B.